Effects of Ag on the Microstructures and Mechanical Properties of Al-Mg Alloys

Haitao Zhang and Bo Zhang

Abstract

The new type 5083 aluminum alloy can be strengthened by heat treatment with the addition of 0.6 wt% Ag. Ag increased the stability of G.P. zones which provided nucleation sites for β″ phase. β″ phase had an ordered cubic $L1_2$ type crystal structure with a lattice parameter of a = 0.408 nm and was primary strengthening phase in the new type 5083 aluminum alloy when aged at 160 °C. The tensile strength of the peak-aged stages of the alloy was 448.9 MPa and the yield strength was 272.8 MPa which increased 39.9 and 88.3 MPa than the as-quenched alloy respectively. The precipitate phase at the over-aged stages was T phase which was body centered cubic structure with a composition of $Mg_{32}(Ag,Al)_{49}$.

Keywords

5083 • Ag • β″ phase • Strength • Peak-aged stages

Introduction

5xxx series aluminum alloy is widely used in the fields of ship and welded structural parts because of its low density, high tensile strength and excellent corrosion resistance [1]. But the alloy can not strengthen by heat treatment and the main strengthening effects of the alloy comes from solid solution strengthening and strain hardening. Thought the strength of the alloy can be improved by increasing the content of Mg, the β phase precipitated along grain boundaries and the corrosion resistance of the alloy decreased when the content of Mg exceeded 3 wt%. Therefore, the strength of the alloy was greatly limited.

It has been reported that Ag can improve the strength of Al-Cu-Mg alloy in the aging process due to the formation of Mg-Ag co-clusters [2]. In Al-Mg alloy, the effect of Ag on the precipitate phases and precipitate sequence were also studied by some researchers. It was already found that small amounts of Ag can induce age-hardening in Al-5 wt% Mg alloy when aged at 150 °C [3]. The strengthening phase was thought as T phase ($Mg_{32}(Al, Ag)_{49}$) in Al-Mg-Ag alloy because the cell closely resembles those ternary phase of Al_6CuMg_4 and $Mg_{32}(Al, Zn)_{49}$ [4]. But the evidences were deficiency due to the restriction of detection technology at that times. The purpose of present work was to investigate the aging hardening response of the low-magnesium content 5083 aluminum alloy with the addition of 0.6 wt% Ag. The precipitation sequences and the relationship between precipitate particles and mechanical properties were discussed in this passage.

Experimental

Alloy ingots of the nominal composition Al-4.5 wt% Mg-0.7 wt% Mn-0.1 wt% Cr-0.15 wt% Zr-(0.6 wt% Ag) were prepared by medium frequency furnace using 99.99 wt% pure Al, 99.99 wt% Mg, 99.99 wt% pure Ag,Mn agent and Cr agent as well as Al+10 wt% Zr master alloy. The size of the ingot was 165 mm × 100 mm × 28 mm. After homogenizing for 24 h at 500 °C, surfaces of the ingot were scalped each side. Then the ingot was hot rolling at 450 °C to 6 mm and cold rolling to 2 mm. After rolling, the solution treatment (ST) was conducted at 500 °C for 2 h followed by water quenching. Subsequent aging treatments were carried out for 0–32 h at 120, 160, 210 and 270 °C respectively.

The Leica DMI5000M type optical microscope (OM) and ULTRA PLUS type scanning electron microscope (SEM) was used to analysis the microstructures of the alloy. The crystalline grain was observed on the Leica DMI5000M

H. Zhang (✉)
Key Lab of Electromagnetic Processing of Materials, Ministry of Education, Northeastern University, Shenyang 110004, Liaoning, China
e-mail: haitao_zhang@epm.neu.edu.cn

B. Zhang
China Hongqiao Group Limited, Huixian 256200, China
e-mail: zhangbo@hongqiaochina.com

C. Chesonis (ed.), *Light Metals 2019*, The Minerals, Metals & Materials Series,
https://doi.org/10.1007/978-3-030-05864-7_63

type optical microscope under polarized light. All specimens for transmission electron microscopy (TEM) were punched mechanically as discs of 3 mm diameter from the strips of 0.08 mm thickness. These disc samples were then thinned to perforate by a twin-jet electro polishing technique. The electrolyte was a solution of 33 vol.% HNO_3 and 67 vol.% CH_3OH. The temperature was from −20 to −30 °C. The voltage was 12–15 V and the current was 50–70 mA. The morphologies of precipitates and diffraction patterns were observed using Tecnai $G^2$20 type TEM and JEM-ARM200F type TEM at an accelerating voltage of 200 kV.

Sample micro-hardness was measured using Vickers hardness instrument, at a load of 5 kg and dwell times of 15 S. The micro-hardness value of each sample was the average of 7 data points. Tensile tests were carried out using CSS-44100 type universal testing machine with a crosshead speed of 2 mm/min. The tensile properties for each sample were the average of three measurements.

Results

Precipitation Hardening Response and Precipitation Sequence

Figure 1 shows the hardness curves of the alloys aged for 0–32 h at 120, 160, 210 and 270 °C respectively. As we can see from Fig. 1a, the hardness value of the Ag-free alloy changed little with the increasing of aging times and temperature. However, the hardness of the Ag-bearing alloy varied obviously in aging process. The higher the temperature, the faster the hardness increased and the shorter the time reached peak hardness. This implies that the aging strengthening effect of the Al-Mg-Ag-Mn–Cr-Zr alloy was remarkable. In the aging process, the increasing of hardness was related to the precipitate particles. The driving force of nuclear of the precipitate particles increased with the aging temperatures and so as the precipitate rate. When the alloy aged at 120 °C, the precipitate rate was lower and the alloy did not reach peak-hardness stages when aged for 32 h. With the improving of aging temperature, the alloy reached peak-hardness at 24, 16, and 2 h respectively when aged at 160, 210 and 270 °C. The maximum hardness value was 117.3 HV when the alloy aged for 24 h at 160 °C by comparing the peak hardness of the alloy aged at different temperatures.

Figure 2a presents bright field (BF) image of Ag-free alloy aged for 4 h at 160 °C. At the under-aged stages, the microstructure contains massive dislocation structure, forming dislocation tangle. There is no precipitated phase in the matrix. When the alloy aged for 24 h at 160 °C, the amount of dislocations decreased due to the low-temperature recovery. At the over-aged stages, some lath-shaped particles β′ phase (Al_3Mg_2) appeared in the matrix.

Figure 3 shows the bright-field (BF) TEM micrograph of the Ag-bearing alloy in different aging conditions. For the as-quenched sample, only coarse-scale Al_6(Mn, Fe) or Mg_2Si particles existed in the matrix and the fine dispersions almost dissolved as shown in Fig. 3a. At the under-aged stages, many dispersions can be observed in the microstructures of the alloy. These particles nucleated homogeneously from the supersaturated solid solution and distributed in the matrix uniformly. At the peak-aged stages, in Fig. 3c, the size of the particles was slightly bigger than that of under-aged stages. The corresponding selected area electron diffraction (SAED) patterns are shown in Fig. 3e and f. The electron beam was approximately parallel to (e) $[110]_{\alpha}$ and (f) $[111]_{\alpha}$. The results indicated that these uniformly distributed dispersions had an ordered cubic $L1_2$ type crystal structure with a lattice parameter of a = 0.408 nm. It was fully consistent with β″ phase in Al-Mg alloy [5]. However, due to the clusters of Ag atoms in the particles, the component of the β″ phase can be summarized as Al_3(Mg, Ag) rather than Al_3Mg. At the over-aged stages, the dimension of the precipitates increased and transformed to rod-like T phase as shown in Fig. 3d.

Table 1 shows the mechanical properties of as-quenched states and the peak-aged stages of the alloy respectively. The tensile strength of the peak-aged stages of the alloy was

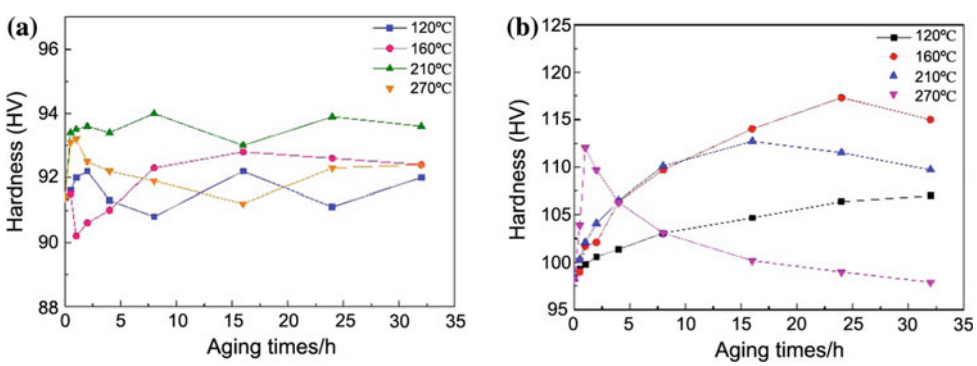

Fig. 1 Hardness curves of the alloys without (**a**) and with (**b**) Ag addition

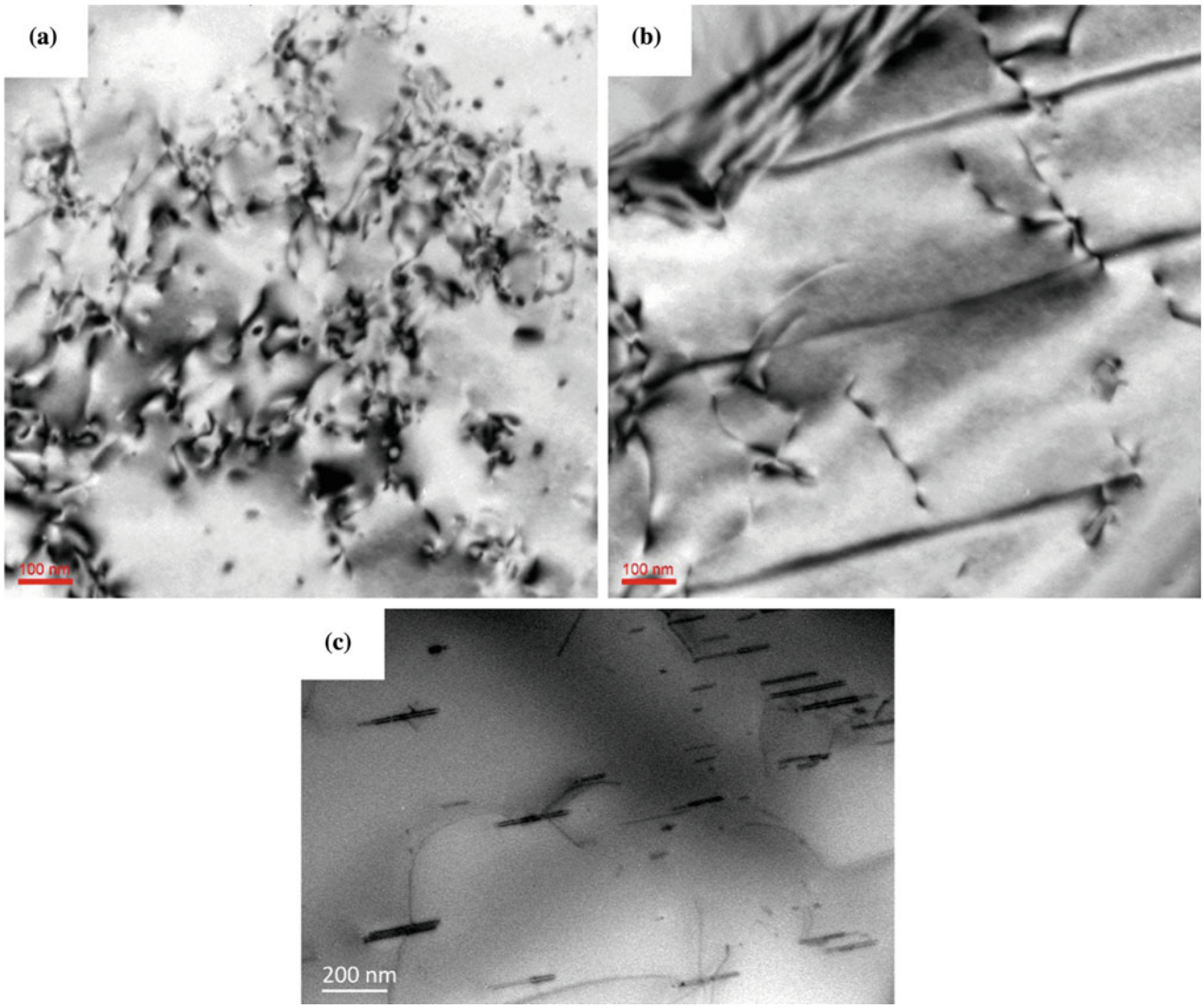

Fig. 2 Bright-field (BF) TEM micrographs of Ag-free alloy aged at 160 °C for **a** 4 h; **b** 24 h; **c** 36 h

448.9 MPa and the yield strength was 272.8 MPa which increased 39.9 MPa and 88.3 MPa than the as-quenched alloy respectively. This is mainly because the fine-scale uniformly distributed β″ phases can hinder the motion of dislocations effectively and the coherent strain energy existed between the β″ phases and Al-matrix. The extensibility of the alloy at the peak-aged stages declined slightly than the as-quenched alloy and still exhibited fine plasticity.

Discussion

As shown in Fig. 1, the hardness of the new type 5083 aluminum alloy has a remarkable improvement in the aging process. When the alloy aged at 160 °C, the hardness of the peak-aged stages of the alloy increased 19 HV than the as-quenched alloy. This is mainly because the precipitation of fine-scale particles as presented in Fig. 2c. It was known that 5xxx series aluminum alloy can not strengthen by heat-treatment because of the instability of G.P. zones and the absence of nucleation sites for transition phases. For Al-Mg alloy, due to the nearest atomic distance of Al is 2.862 Å and Mg is 3.196 Å, the elastic strain energy between G.P. zones and aluminum matrix was large and Gibbs free energy improved. Thus G.P. zones can not exist in the matrix stably and the nucleation sites for precipitate particles were absent.

However, for the new type 5083 aluminum alloy, many fine-scale particles precipitate in the matrix uniformly during aging. It reflects that Ag had a positive effect on the formation of stable G.P. zones and β″ phases. The concentration of vacancies and the super saturation of solute atoms increased in the supersaturated solid solution with the addition of 0.6 wt% Ag. So the nucleation power of G.P. zones increased. Besides, as reported in Al-Cu-Mg-Ag

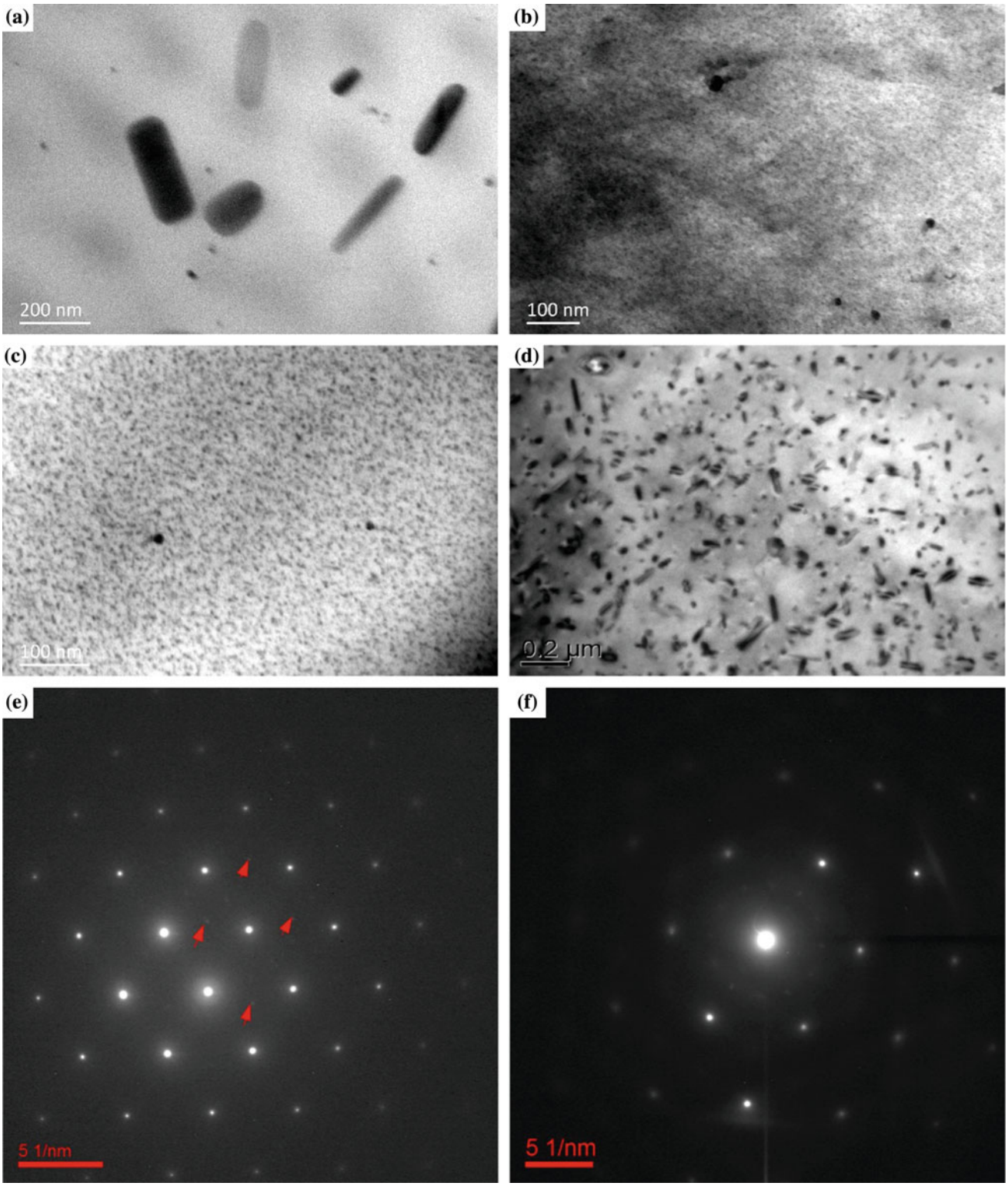

Fig. 3 Bright-field (BF) TEM micrographs of the Ag-containing alloy for **a** as-quenched; **b** aged for 4 h at 160 °C; **c** aged for 24 h at 160 °C; **d** aged for 32 h at 160 °C. **e** and **f**: the SAED patterns of **c** along $[110]_\alpha$ and $[111]_\alpha$ respectively

alloy, Ag is effectively trap to Mg atoms, resulting in the formation of numerous Mg-Ag co-cluster [6, 7]. Thus Ag modified the precipitation process of the new type 5083 aluminum alloy from the earliest stages of the decomposition through a preferred Mg-Ag interaction. At the pre-aging stages, the supersaturated vacancies promoted the diffusion

Table 1 Mechanical properties of as-quenched alloy and the alloy aged for 24 h at 160 °C respectively

Sample	Tensile strength/MPa	Yield strength/MPa	Extensibility/%
As-quenched	409	184.5	26.2
160 °C/24 h	448.9	272.8	21.6

of solute atoms, forming Mg-Ag G.P. zones. On the other hand, owing to the atomic radii of Al and Ag differ by only 0.5%, Ag reduced the elastic strain energy between G.P. zones and Al-matrix. So the uniformly dispersed G.P. zones can exist stably at the pre-aging stages.

At the peak-aged stage, the G.P. zones transformed to fine-scale β″ phases which distributed in the matrix uniformly. It reflects that the β″ phases were homogeneous nucleation from G.P. zones. β″ phases were coherent with the matrix, but due to the difference of atom size between solute atoms and Al-matrix, the lattice distortions and elastic strain zones within the particles can be detected. The component of the β″ phase can be summarized as Al_3(Mg, Ag) rather than Al_3Mg owing to the obvious Mg-Ag clusters within the particles. On the one hand, the fine-scale particles can inhibit the movement of the dislocations and so effectively strengthen the alloy. On the other hand, the elastic strain energy between precipitate dispersions and matrix can improve the strength of the alloy in a certain extent. Thus at this stages, the alloy reached peak-hardness when aged at 160 °C. The mechanical properties of the peak-hardness stages of the alloy had a visible improvement than the as-quenched alloy. The tensile strength increased 39.9 MPa and the yield strength increased 88.3 MPa respectively. It mainly contributes to the pinning of β″ phase in dislocation motion and the elastic strain energy between the precipitate particles and Al-matrix. Besides, due to the fine equiaxed grains forming in the process of solution treatment, the alloy exhibited fine plasticity in both as-quenched alloy and peak-aged stages of the alloy.

At the over-aged stage, as shown in Fig. 3d, many coarse-scale rod-like particles precipitated in the matrix sparsely. The coherent β″ phases transformed to T phases which were incoherent with the matrix. The size of the precipitate particles increased and the amount of the particles declined. During coarsening, large precipitates grew on the expense of small precipitates in the matrix in order to reduce the interfacial energy in the material [8]. The microstructures of the alloy are always unstable if the interfacial free energy is not a minimum. Therefore, a high density of small precipitates tends to coarsen into a lower density of larger particles with a smaller total interfacial area [9]. it has been reported that T phase was metastable by many researchers [10]. If the aging time was prolonged or the aging temperature continually improved, it is not sure whether T phase may transform to equilibrium β phase (Al_3Mg_2) or not.

Conclusion

Effect of Ag on the microstructures and mechanical properties of 5083 aluminum alloy was investigated in this passage. The new type 5083 aluminum alloy can be strengthened by heat treatment with the addition of 0.6 wt% Ag. Ag increased the stability of G.P. zones which provided nucleation sites for β″ phase. β″ phase had an ordered cubic $L1_2$ type crystal structure with a lattice parameter of a = 0.408 nm and was primary strengthening phase in the new type 5083 aluminum alloy when aged at 160 °C. The tensile strength of the peak-aged stages of the alloy was 448.9 MPa and the yield strength was 272.8 MPa which increased 39.9 and 88.3 MPa than the as-quenched alloy respectively. The precipitates at the over-aged stages was T phase which was body centered cubic structure with a composition of $Mg_{32}(Ag,Al)_{49}$.

References

1. G. B. Burger, A. K. Gupta, P. W. Jeffrey, D. J. Lloyd (1995) Microstructural control of aluminum sheet used in automotive applications, Materials Characterization. 35: 23–29.
2. S. P. Ringer, K. Hono (2000) Microstructural evolution and age hardening in aluminum alloys: Atom probe field-ion microscopy and transmission electron microscopy studies, Materials Characterization, 44:101–131.
3. I. J. Polmear, K. R. Sargant, Enhanced age-hardening in aluminum-magnesium alloys, Nature, 200 (1963) 669–670.
4. M. J. Wheeler, G. Blankenburgs, R. W. Staddon (1965) Evidence for a ternary phase in the aluminum-magnesium-silver system, Nature, 207: 746–747.
5. M. J. Starink, A. M. Zahra (1998) β′ and β precipitation in an Al-Mg alloy studied by DSC and TEM, Acta Materialia, 46: 3381–3397.
6. J. Howe (1994) Analytical transmission electron microscopy analysis of Ag and Mg segregation to {111} θ precipitate plates in an Al-Cu-Mg-Ag alloy, Philosophical Magazine Letters, 70: 111–120.
7. K. Hono, M. Murayama, L. Reich (1999) Clustering and segregation of Mg and Ag atoms during the precipitation processes in Al(-Li)-Cu-Mg-Ag alloys, Revista De Metalurgia.
8. R. M. Aikin Jr, M. R. Plichta (1990) Concurrent size and shape coarsening of γ′ in Al-Ag, Acta Metall, 38: 77–93.
9. S. Senapati (2005) Evolution of lamellar structures in Al-Ag alloys.
10. M. Kubota, J. F. Nie, B. C. Muddle (2005) Identification of metastable rod-like particles in an isothermally aged Al-10 Mg-0.5Ag (mass%) alloy, Materials Transactions, 46: 1288–1294.